

# Ultra-thin SiO<sub>2</sub> on Si IX: absolute measurements of the amount of silicon oxide as a thickness of SiO<sub>2</sub> on Si

M. P. Seah,<sup>a\*</sup> W. E. S. Unger,<sup>b</sup> Hai Wang,<sup>c</sup> W. Jordaan,<sup>d</sup> Th. Gross,<sup>b</sup> J. A. Dura,<sup>e</sup> Dae Won Moon,<sup>f</sup> P. Totarong,<sup>g</sup> M. Krumrey,<sup>h</sup> R. Hauert<sup>i</sup> and Mo Zhiqiang<sup>j</sup>

Results from a study conducted between National Metrology Institutes (NMIs) for the measurements of the absolute thicknesses of ultra-thin layers of SiO<sub>2</sub> on Si are reported. These results are from a key comparison and associated pilot study under the auspices of the Consultative Committee for Amount of Substance. 'Amount of substance' may be expressed in many ways, and here the measurand is the thickness of the silicon oxide layers with nominal thicknesses in the range 1.5–8 nm on Si substrates, expressed as the thickness of SiO<sub>2</sub>. Separate samples were provided to each institute in containers that limited the carbonaceous contamination to approximately <0.3 nm. The SiO<sub>2</sub> samples were of ultra-thin on (100) and (111) orientated wafers of Si. The measurements from the laboratories which participated in the study were conducted using ellipsometry, neutron reflectivity, X-ray photoelectron spectroscopy or X-ray reflectivity, guided by the protocol developed in an earlier pilot study. A very minor correction was made in the different samples that each laboratory received. Where appropriate, method offset values attributed to the effects of contaminations, from the earlier pilot study, were subtracted. Values for the key comparison reference values (agreed best values from a Consultative Committee study) and their associated uncertainties for these samples are then made from the weighted means and the expanded weighted standard deviations of the means of these data. These results show a dramatic improvement on previous comparisons, leading to 95% uncertainties in the range 0.09–0.27 nm, equivalent to 0.4–1.0 monolayers over the 1.5–8.0 nm nominal thickness range studied. If the sample-to-sample uncertainty is reduced from its maximum estimate to the most likely value, these uncertainties reduce to 0.05–0.25 nm or ~1.4% relative standard uncertainties. The best results achieve ~1% relative standard uncertainty. It is concluded that XPS has now been made fully traceable to the SI, for ultra-thin thermal SiO<sub>2</sub> on Si layers, by calibration using wavelength methods in an approach that may be extended to other material systems. © Crown copyright 2009. Reproduced with the permission of Her Majesty's Stationery Office. Published by John Wiley & Sons, Ltd.

**Keywords:** attenuation length; calibration; silicon dioxide; thickness; ultra-thin oxide

## Introduction

This study concludes the first detailed metrological study on the thicknesses of ultra-thin films conducted between National Metrology Institutes (NMIs). The use of ultra-thin films in industry today has grown significantly, covering sectors as widely different as microelectronics and sensors to bioengineering and drug delivery systems. For efficiency, quality and yield reasons, these films need to be controlled and characterised. Here, the term 'ultra-thin' is applied to films less than 10-nm thickness (i.e. less than 40 atom layers). There are many analytical methods that provide a detailed analysis of different aspects of these films, but many, although having good precision, lack traceability to a quantitative measure. Often, unfortunately, those methods providing much detailed information to characterise films, such as static secondary ion mass spectrometry (SIMS), have the poorest traceability to amount of substance as expressed here by the thickness of a given material.

In the field of length measurement, in contrast, there are many methods that have excellent traceability for measuring film thicknesses. However, these methods exhibit greater and greater uncertainties as the thickness reduces until, eventually, the thickness is too small to provide useful data without a detailed knowledge of the sample.

\* Correspondence to: M. P. Seah, Quality of Life Division, National Physical Laboratory (NPL), Teddington, Middlesex TW11 0LW, UK. E-mail: martin.seah@npl.co.uk

a Quality of Life Division, National Physical Laboratory (NPL), Teddington, Middlesex TW11 0LW, UK

b Bundesanstalt fuer Materialforschung und -pruefung (BAM), D-12200 Berlin, Germany

c Physicochemical and Chemical Engineering Division, National Research Center for Certified Reference Materials (NRCCRM), No. 18, Bei Sanhuan Donglu, Chaoyang District, Beijing 100013, China

d National Metrology Institute of South Africa, Surface and Microanalysis (NMISA), Private Bag X34, Lynnwood Ridge, Pretoria 0040, South Africa

e NIST-Center for Neutron Research, 100 Bureau Dr. MS 8562, Building 235, Room E124, Gaithersburg, MD 20899-8562, USA

f Division of Chemical Metrology and Materials Evaluation, Korea Research Institute of Standards and Science (KRISS), Doryong-1, Yusong, Taejeon 305-600, Republic of Korea

g National Institute of Metrology, Thailand (NIMT), 3/4-5 Moo 3 Tumbon Klong 5, Klong Luang, Pathumthanee, 12120 Thailand and Thai Microelectronics Center, National Electronics and Computer Technology Center, National Sciences and Technology Development Agency, Ministry of Science and Technology, 51/4 Moo 1, Wang Takien District, Amphur Mueng Chachoengsao 24000 Thailand

h Physikalisch-Technische Bundesanstalt (PTB), Abbestraße 2-12, D-10587 Berlin, Germany

This study focuses on the system of SiO<sub>2</sub> on Si as it is technologically important, impacts a number of fields, is a basis for reference materials and has a very wide publication base. The ultra-thin film that is most thoroughly understood and characterised is that of thermal SiO<sub>2</sub> grown on pure Si wafers. Much work has been completed, in the past, on films 20–200 nm thick, but, today, the interest focuses on the range below 8 nm. Material samples are robust, stable, reproducible and widely available. For these reasons and because high-quality material was being grown in expert laboratories, the present intercomparison is focused on the thermal oxide of silicon in the thickness range 1.5–8 nm. Silicon oxides made by other routes, such as polishing or plasma deposition, may have different stoichiometries, densities, defect levels and other properties. The extent that this study directly illuminates their measurement depends on how closely their properties match those of the thermal oxide.

Thermal oxides are the basis of many semiconductor technologies, where the International Technology Roadmap for Semiconductors (ITRS)<sup>[1]</sup> indicates a need for the measurement of ultra-thin gate oxides at a control standard uncertainty of just over 1%. Prior to the pilot study for this work,<sup>[2]</sup> the standard uncertainty for measurements in a given laboratory seemed to be somewhere in the range 15–50%. Improvements in the accuracy for the quantity of oxide measured on Si is also important for the developing Avogadro project based on single crystal Si spheres,<sup>[3,4]</sup> the surface of which will be covered with an oxide together with the adventitious carbon, hydrocarbon and water that have been seen by analysts in the present work. Unfortunately, with samples exposed to the atmosphere, different contaminations react with the surface and form surface layers that may be chemisorbed, and difficult to remove, as well as those that are physisorbed and largely removable. The use of vacuum is, unfortunately, not such a panacea for maintaining a clean surface since in a good, ultra-high vacuum of 10<sup>−9</sup> millibar, a monolayer of the ambient gas may adsorb in around 30 min.<sup>[5]</sup> At our mid-range of thickness of 3 nm, one monolayer is a change of 8% unless it can be isolated in the analysis.

Full details of the background to this work may be found in the report to the earlier pilot study (P38) to this work<sup>[2]</sup> where many analytical methods are presented. The present work builds on that to bring the study to definitive conclusions.

The pilot study P38<sup>[2]</sup> has already shown that the historical view on the hierarchy of the accuracies of relevant methods required revision and that some methods that were thought to be good turned out to be less good and *vice versa*. This resulted in a much improved understanding of the uncertainty contributions in most analytical methods and hence, in several cases, to their further development. It has also resulted in an improved understanding of the measurement methods themselves and hence to an improved infrastructure for the general measurement of ultra-thin films of this and of other compositions. Prior to these studies, the inter-laboratory, inter-method scatter range approached 100% at ~4 nm film thicknesses.<sup>[6]</sup> In the pilot study P38,<sup>[2]</sup> offsets attributed to surface contaminations of water and carbonaceous matter were identified in a range of methods. These appeared to be consistent but unique to each method and laboratory. Thus, thickness differences from each laboratory showed very good consistency. This was a major improvement. The present report on the final stages for the absolute thicknesses is based on the results from the key comparison, K32, and the associated pilot study, P84,<sup>[7]</sup> that follow the earlier pilot study P38.<sup>[2]</sup>

In pilot studies, any expert laboratory may be involved in order to provide the widest and most complete evaluation of

relevant issues. In key comparisons, only NMIs are involved since it is through them that the international system of units (SI) has traceability in each country. Traceability, to be remembered, is defined as ‘property of the result of a measurement or the value of a standard whereby it can be related to stated references, usually national or international standards, through an unbroken chain of comparisons all having stated uncertainties’<sup>[8]</sup> i.e. there is an unbroken chain linking the stated uncertainty of a given result to the SI system. This SI system is promulgated further down the line nationally through the NMIs and validated through international comparisons under the auspices of the Consultative Committees to internationally agreed standards. The concept of uncertainty is generally well understood, but it must be remembered that each parameter involved in generating a result will have associated uncertainties and these may or may not be significant. Each equation used will, itself, only be valid to a certain level of uncertainty. Additionally, these uncertainties will be composed of one or more type A (random) and one or more type B (systematic) uncertainties. Lastly, the uncertainties themselves will have uncertainty and care must be exercised when considering their combination and also their expansion from standard uncertainties at a confidence level of 68% to those relevant for, say, the 95% confidence level often associated with certificates from NMIs.

Above, pilot studies and key comparisons are mentioned. An important difference is that key comparison results are the definitive results from NMIs and only these results are used for the key comparison reference values (KCRVs) used internationally to determine derived equivalences. The KCRVs are the best estimates of the values of physical quantities as deduced from the measurements from participating NMIs, taking their uncertainties into account at 95% confidence levels. The difference between the results from each NMI and that of the KCRV is the ‘Degree of Equivalence’ for that country and is used when comparisons are required at the highest accuracy. Analysts working within quality systems, those accredited to ISO 17025<sup>[9]</sup> and those involved in commerce where these measurements are provided, will already be aware of the issues of traceability and uncertainty, but they may be less aware of KCRVs which underpin the values of parameters or reference material properties that they are using. Absolute thicknesses, rather than thickness differences, are now consistent at the required level indicated in the ITRS.

## The Measurand and the Samples

The measurand in this study is the thickness of the silicon oxide layer on each of a total of nine samples of nominal thicknesses in the range 1.5–8 nm on (100) and (111) Si substrates, expressed as the thickness of SiO<sub>2</sub>. The participants in the study were free to choose their analytical method in order to achieve the highest accuracy in their laboratories. Eight institutes provided data that are included in the KCRVs and two institutes provided data solely for the associated pilot study, P84. In Germany, two institutes participated in K32 in different thickness ranges, other data by them appearing in the associated pilot study.

The material for K32 and P84 is from batches made in European and US facilities with those for the pilot study P38. They were

i Swiss Federal Laboratories for Materials Testing and Research (EMPA), Überlandstr. 129, CH-8600 Dübendorf, Switzerland

j Chemical and Materials, PSB Corp., 1 Science Park Drive, Singapore 118221

grown by thermal oxidation in very clean furnaces designed for high-quality gate oxides on Si wafers. After production, the US material was provided in a sealed dust-free container to the European facility where all of the samples were mapped for the oxide thickness using a Philips PZ 2000 ellipsometer designed for production-line thickness determination. This instrument provided maps with a precision around 0.002 nm, allowing samples to be selected from regions that were homogeneous to within  $\pm 1\%$ . An example of a map, in colour, is given in plate 1 of Seah and White.<sup>[10]</sup> That particular sample shows a central region of 80-mm diameter that could have been used in these studies but other samples were more homogeneous and so were used instead. Analysis by X-ray photoelectron spectroscopy (XPS) shows that these ellipsometry maps are accurate, as discussed below, for relative thicknesses in each wafer. The production technology has been improved as a result of this mapping.

In order to ensure the highest accuracy, the thickness of each sample provided to analysts was recorded for its position in each ellipsometry map. The nine thicknesses chosen for this study were five of (100) Si, being nominal thicknesses 1.5, 2, 3, 4 and 8 nm, together with four of (111) Si, being nominal thicknesses 2, 3, 5 and 6 nm. The (100) Si wafers were cut into squares bounded by the (111) planes defining the [110] directions, whereas the (111) wafers were cut into triangles bounded by the same planes and directions.<sup>[11]</sup>

After cutting, the samples were blown with an argon jet to remove cutting debris, and then most of the carbonaceous contamination was removed by an overnight (16 h) soak in high-purity isopropyl alcohol (IPA), ultrasonic agitation in fresh IPA and blow drying with an argon jet. In this way, the remaining carbonaceous contamination could be reduced from, typically, 0.64 nm to a layer typically with 0.12-nm thickness.<sup>[12]</sup> Cleaning to remove this final layer requires more aggressive methods. Ultra violet with ozone achieves this but at the expense of affecting the oxide. These carbonaceous thicknesses were measured by XPS with undefined uncertainties. Subsequent XPS measurements of storage in different containers showed that there was then an additional carbonaceous contamination thickness that increased approximately with the square root of time over the first 100 days and that polypropylene 'Fluoroware®' would typically keep the contamination below 0.25 nm for 3 months.<sup>[12]</sup> Fluoroware is commonly used for semiconductor wafer containers. Samples were therefore supplied in these containers, only to be opened just prior to use.

In addition to the growth of the carbonaceous contamination, repeated XPS measurements of the oxide thicknesses have been made for one set of the samples stored in the Fluoroware containers after 6 months. The average increase in the oxide thickness over the 6 months, as measured by XPS, is  $0.001 \pm 0.059 \text{ nm}^{[2]}$  i.e. there was no change between the repeatedly taken measurements. The samples are thus assumed to be stable for the period of the measurements reported here.

## The Participants' Measurement Procedures

All participants have submitted results with uncertainties except PSB corp., who were in the pilot study, P84. PSB provided repeatability data. In the following paragraphs, the methods are summarised.

For the key comparison K32, BAM, KRISS and NPL used XPS with Mg K $\alpha$  X-rays at the magic angle and the NPL reference

geometry with  $R_o = 0.9329$  and  $L = 2.996 \text{ nm}$ , as cited by Seah and Spencer.<sup>[13]</sup> XPS is always conducted in ultra-high vacuum. The instruments used were a Kratos Axis Ultra DLD, a Scienta SES-100 electron spectrometer and a VG Scientific ESCALAB II with a 210 analyser, respectively. NRCCRM used a VG Scientific ESCALAB 220i-XL XPS similarly but with  $L = 2.964 \text{ nm}$ , as cited by Seah *et al.*<sup>[2]</sup> NMISA used a Physical Electronics Quantum 2000 XPS similarly but with Al K $\alpha$  X-rays and  $L = 3.485 \text{ nm}$ , as cited by Seah and Spencer.<sup>[13]</sup> Example spectra are given by Seah and Spencer.<sup>[11]</sup>

NIST used neutron reflectometry (NR) in vacuum with cold neutrons<sup>[14]</sup> of wavelength 0.475 nm, as discussed by Seah *et al.*<sup>[2]</sup> and more generally by Dura *et al.*<sup>[15]</sup> Example reflectivity curves are given in the two studies.

PTB used X-ray reflectometry (XRR) at BESSY II in vacuum at a photon energy of 1841 eV, chosen for the high contrast between SiO<sub>2</sub> and Si, combined with X-ray fluorescence (XRF) measurements at a photon energy of 480 eV for high carbon sensitivity. Example reflectivity curves are given by Seah *et al.*<sup>[2]</sup>

NIMT and the Thai Microelectronics Center (TMEC) used ellipsometry in ambient air with a Rudolph Technologies dual wavelength (HeNe laser for 633-nm beam and 780-nm laser diode) focused beam FE III Focus Ellipsometer for simultaneous multi-angle measurements with in-built data processing and calibration. For the KCRV data, the samples were heated to 350 °C for 10–15 min and then allowed to cool for 10–15 min prior to measurement.

For the pilot study P84, BAM and PTB used the same conditions as above. EMPA used XPS with Al K $\alpha$  X-rays and the NPL reference geometry with  $R_o = 0.933$  and  $L = 3.448 \text{ nm}$ , as cited by Seah *et al.*<sup>[2]</sup> PSB corp. used XPS with Al K $\alpha$  X-rays at an emission angle of 45° with  $R_o = 0.896$  determined experimentally and  $L = 3.448 \text{ nm}$ .

## Results

The values of the thicknesses and their associated uncertainties at a 95% level of confidence were provided. They and their associated tables are given in Ref. [7]. For the comparison of data, two adjustments are required. First, each of the individual samples has its own thickness, as noted above, characterised by the ellipsometry map measurements just after manufacture. For comparison of the laboratories with each other, the differences in the thicknesses of each sample from a reference sample need to be subtracted and the additional uncertainty associated with this adjustment added. These differences have been measured by ellipsometry with a precision standard deviation of 0.002 nm. The average of the total ranges for these samples from their median is less than 0.8% of the absolute thickness. This small value was obtained by careful selection of the material available. These differences, with a mean magnitude of 0.02 nm, have an associated uncertainty at 95% confidence of 0.06 nm. This uncertainty arises from comparisons of pairs of samples and includes the two separate ellipsometric measurements and the two XPS measurements required to confirm each thickness difference. The 0.06 nm difference is probably an overestimate, as it is unlikely that the constant thickness areas from ellipsometry arose from areas where any reduction in the SiO<sub>2</sub> thickness had been fortuitously compensated by extra contamination to mask this reduction. However, this 0.06 nm was added in quadrature to the uncertainties given by each analyst before plotting calculating

comparative data in Ref. [7]. It is more likely that this value should be significantly smaller and so we investigate that below.

Second, corrections need to be applied for the effects of surface contaminations currently thought to be the source of the different offsets seen in thicknesses measured by the different methods. The final carbonaceous layer is thought to be a catalytically reduced carbon layer with sp<sup>2</sup> bonding.<sup>[16]</sup> It is known that adsorbing hydrocarbons may catalytically dehydrogenate at a clean SiO<sub>2</sub> surface. This continues until the active sites are all covered with a layer of 'coke'. Thus, the adventitious contamination is likely to include a thin carbon layer of the order of a fraction of a monolayer of carbon (0.2 nm), covered with a thin hydrocarbon layer whose thickness grows with the square root of time.<sup>[12]</sup> Added to this layer will be both chemisorbed and physisorbed water and the extent of that water will, for measurements in air, depend on the relative humidity<sup>[17–19]</sup>, and, maybe, the extent of hydrocarbon uptake. Measurements<sup>[17–19]</sup> indicate that the physisorbed water thickness could be between 0.05 and 0.3 nm. Azuma *et al.*<sup>[20]</sup> show, using XRR, by fitting with a two-layer model of water and oxide instead of a one-layer model of the oxide that the full extent of the water layer in air is 0.55–0.67 nm for thermal oxides of similar thicknesses to those measured here. Furthermore, they show using thermal desorption spectrometry that the water requires 800 °C for removal in the classical  $\alpha$ ,  $\beta_1$  and  $\beta_2$  physisorption and chemisorption states.

Chemical shift data for the C 1s peak from XPS are consistent with the carbon-based part of this contamination model, but hydrogen is not directly observable by any of these methods. Data from BAM confirm the dehydrogenated layer with observations by near edge X-ray absorption fine structure spectroscopy (NEXAFS) which show a clear, narrow and intense C 1s  $\rightarrow \pi^*$  resonance of unsaturated carbon species in the spectrum.

NR and XRR simulations show that the above contamination is consistent with the discrepancy, identified in the pilot study P38, between NR and XPS and also between XRR and XPS. The most plausible explanation available for NR and XRR data is that a combination of carbon, hydrocarbons and water creates a contamination layer that has a scattering length density (SLD) or electron density close enough to SiO<sub>2</sub> to be indistinguishable from SiO<sub>2</sub> and that the offsets in the pilot study P38<sup>[2,21]</sup> measure this effect and permit their subtraction. These offsets are given in Table 1. These have been determined from the data given in the pilot study P38,<sup>[2,21]</sup> but, instead of fitting a line and establishing a gradient  $m$  and offset  $c$ , the absolute difference is calculated directly from the same data for each thickness, using the calibrated XPS attenuation length.<sup>[13]</sup> This method is appropriate if the same equipment and data reduction procedures are used in this study as in the pilot study P38. This was not the case for NIMT since NIMT was not part of that study. Fortunately, the ellipsometry method is robust and the offset uncertainties may be evaluated from the experimental standard deviations of the distribution of results and other terms described later. The offset for NIMT is established from the average offset between XPS and ellipsometry results for those responding to the pilot study P38, adjusted for the reduction in contamination that arises from the use, in NIMT, of a hot stage. The uncertainties concern the populations of these distributions.

The thickness values that may be compared are thus the reported values corrected for the small sample-to-sample changes and for the offsets from Table 1 with their 95% confidence uncertainties combined in quadrature. These results are all shown in the formats of Seah *et al.*<sup>[2]</sup> and Cole *et al.*<sup>[6]</sup> in Fig. 1. However, the results are now so close to each other that the detail is no

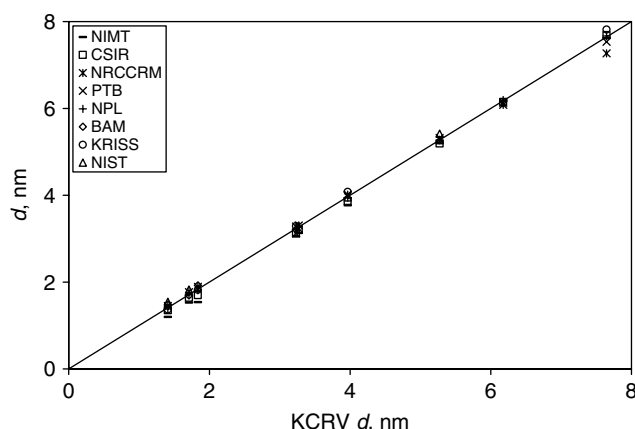


**Figure 1.** Values of thickness for each NMI on the ordinate, corrected to a reference sample, as a function of the weighted average thicknesses from Table 2 on the abscissa.

longer resolvable. Instead, Fig. 2 shows the results for four of the nine samples in greater detail, where the first eight values, reading from the left are for the key comparison laboratories. Complete data are given in Ref. [7]. The laboratories are identified along the abscissa. The laboratory order follows a convention that starts with the laboratory with the overall lowest average value and finishes with that reporting the highest overall average value. This is slightly different from the usual convention in which the order is set differently for each sample. Following the eight key comparison laboratories is a vertical dividing line, followed by the four laboratories in the pilot study P84. In key comparisons, only one designated laboratory in each country can contribute to each measurand. In Germany, there is a separation defined by thickness where BAM measured the three thinnest samples by XPS and PTB the thicker samples by XRR. Other data appear in the associated pilot study. Thus, in Fig. 2(a) and (b), there are values from BAM in K32 and PTB in P84, whereas in Fig. 2(c) and (d) these positions are reversed.

The 0.06-nm uncertainty noted earlier for the sample-to-sample uncertainty propagates through the KCRV uncertainty. The KCRV values and their associated uncertainties at 95% confidence are now calculated from the weighted averages, as shown in Table 2. The expanded uncertainties use  $k$  values, from Student's tables, that are in excess of two to allow for the relevant degrees of freedom.

Two further analyses are interesting at this stage. First, in Fig. 3 the KCRV standard uncertainties,  $u$ , for the (100) and (111) samples, are plotted as a function of the thicknesses and it is clear that there is no significant difference between the (100) and (111) sets, both being described by the equation:

$$u = 0.0106d + 0.024 \text{ nm} \quad (1)$$

**Table 1.** Offsets determined from the data for the pilot study, P38

Institutes	Offset (nm)	$k$ , (no. of results)	$k$ times the standard deviation (nm)
NIMT (ellipsometry)	0.78	2.447 (7)	0.39
PTB (XRR)	0.49	4.303 (3)	0.29
NIST (NR)	0.22	3.182 (4)	0.26



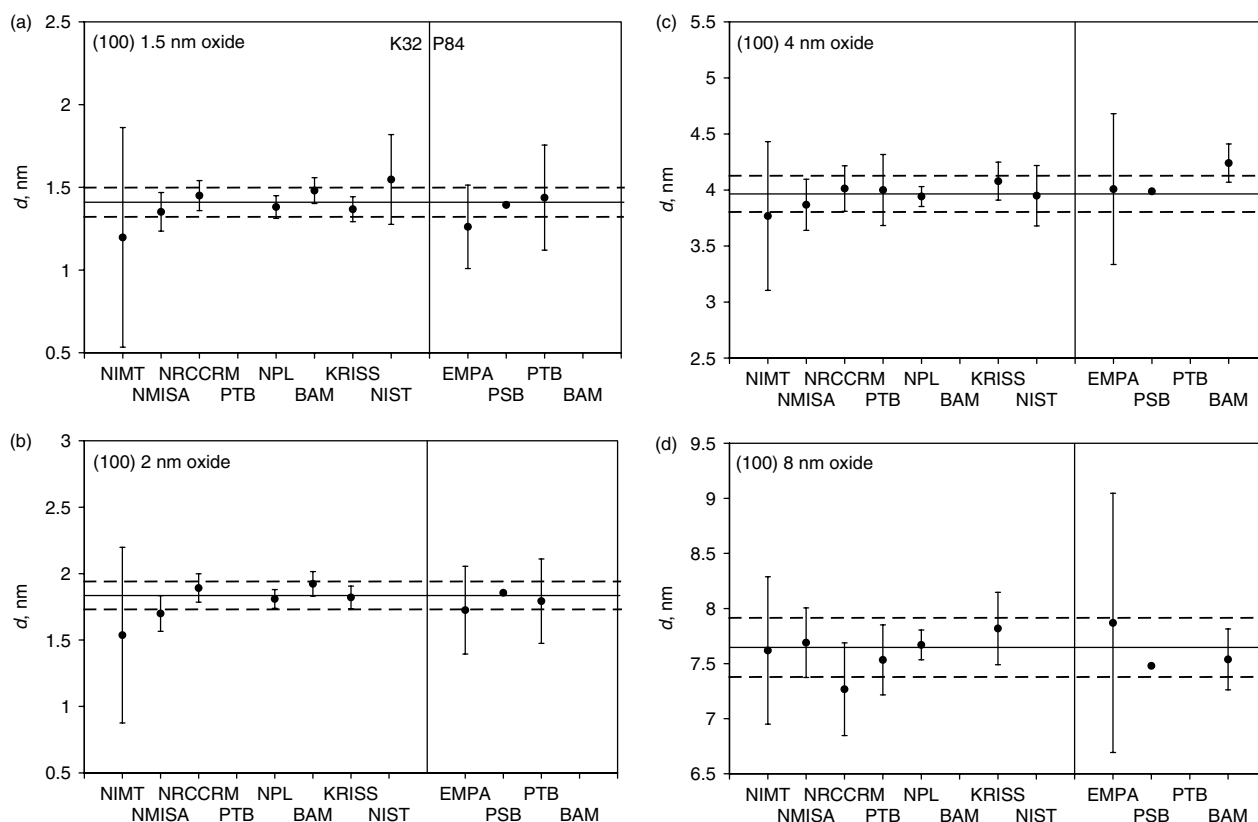


**Figure 2.** Thickness measurements with their uncertainties at 95% confidence from K32, to the left, and P84, to the right. These data are corrected to a reference wafer with the sample-to-sample uncertainty added for intercomparison for the thicknesses of the (100) samples: (a) 1.5 nm, (b) 2 nm, (c) 4 nm and (d) 8 nm. The solid and dashed lines show the KCRV and the 95% confidence intervals from Ref. [7], respectively.

**Table 2.** Key comparison reference values (KCRVs) from the weighted means with the uncertainties for 95% confidence intervals from  $k$  times the standard deviations

Substrate orientation	100					111			
Nominal thickness (nm)	1.5	2	3	4	8	2	3	5	6
Weighted mean, $d_R$ (nm)	1.41	1.84	3.23	3.97	7.65	1.71	3.27	5.27	6.18
$k$ value	2.45	2.57	2.57	2.45	2.57	2.57	2.78	2.57	2.78
Uncertainty at 95% confidence, $U_R$ (nm)	0.09	0.10	0.15	0.16	0.27	0.11	0.18	0.20	0.25

The standard uncertainties are plotted, as there is a systematic difference for the expanded uncertainties where a higher  $k$  value, as shown in Table 2, has been required for the (111) samples than for the (100), there being more results for the latter and hence a lower  $k$  value.

The second useful parameter to calculate is the standard score given by  $z$  where

$$z = \frac{x - \mu}{\sigma} \quad (2)$$

and where  $x$  is the laboratory result with standard uncertainty  $\sigma$ , and  $\mu$  is the KCRV. For the 54 K32 results, the standard deviation of the  $z$  values should be around unity, but it is only 0.67. This value may be low, partly as a result of the use of the over-cautious 0.06-nm value used to define the sample-to-sample uncertainty.

It is likely that the sample-to-sample uncertainty should be defined by the two relevant ellipsometry measurements added in quadrature rather than those as well as the two XPS measurements used to confirm them as discussed in Section 3. In this case, the real sample-to-sample uncertainty at 95% confidence is not

0.06 nm, but 0.006 nm. When recalculating  $\sigma$  and  $\mu$  for each result, the standard deviation of the  $z$  values rises to 0.84. This is still lower than the expected unity and may arise from slightly cautious estimates of uncertainties from laboratories submitting data for such a first intercomparison. Using a sample-to-sample uncertainty value of 0.006 nm and reductions in certain other uncertainties, as described in the analysis of uncertainties in the Appendix, new weighted means may be calculated and the results updated as shown in Fig. 3 where the solid points and the solid line move to the hollow points and the dashed line. This latter fit is described by an excellent result

$$u = 0.0116d + 0.007 \text{ nm} \quad (3)$$

The equivalent revisions of Fig. 2 are shown in Fig. 4. In the full set of data, only 3 of the 54 results with uncertainties now just miss the weighted mean, as expected at 95% confidence, although they do overlap the weighted mean with its uncertainty. Figure 4 is thus probably closer to the truth than Fig. 2, although the latter,

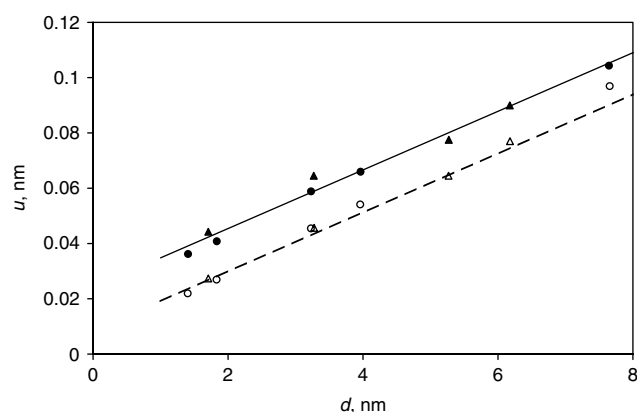


**Figure 3.** Key comparison reference values with their standard uncertainties for the (100) samples [closed circles (●)] and (111) samples [inverted triangles (▲)] with Eqn(1) [solid line (—)]. Below these are the revised values using the reduced uncertainties discussed in the text, (100) samples [open circles (○)] and (111) samples [open triangles (△)] with Eqn (3) [dashed line (---)].

**Table 3.** Offsets determined from the data for the pilot studies, P38 and P84 and the key comparison, K32

Institute	Offset (nm)	k (no. of results)	k times the standard deviation (nm)
PTB (XRR)	0.49	2.201 (12)	0.18
NIST (NR)	0.28	2.365 (8)	0.22

having greater uncertainty, will embody greater confidence and was used in the KCRV analysis.<sup>[7]</sup>

For future work, the present results from NIST and PTB may be used with those from the first pilot study to define their offsets shown in Table 1 more precisely, as shown in Table 3. Here the major gain is through the reduction in the *k* values associated with the significant increase in the number of results.

## Conclusions

In measuring the amount of silicon oxide expressed as a thickness of SiO<sub>2</sub> on Si where the oxide layer is formed by thermal oxidation, significant progress has been made which is sufficient to provide KCRV values with relative standard uncertainties in the range 2.5–1.5% for thermal oxide thicknesses in the range 1.4–7.7 nm, respectively. Individual measurements may have precisions better than 0.5%. Offsets observed in the pilot study P38 and attributed to contaminations have been considered and where necessary, in many cases, removed. This correction improves the uncertainty for absolute thickness measurements. However, where thickness differences are required and where samples can be treated so that the contaminations are effectively the same, significantly lower uncertainties may apply. For oxides prepared by routes other than thermal oxidation, which may have different densities, stoichiometries, surface reactivities or other properties, the input parameters for the various methods may require change.

The uncertainties at 95% confidence, ranging from 0.09 to 0.27 nm as the thickness increases from 1.5 to 8 nm, represent a typical improvement factor of 20 on the situation prior to this overall study. In the context of this result, it is worth remembering

that one monolayer of SiO<sub>2</sub> is only ~0.25 nm. Calculations of the KCRVs from the weighted mean and weighted uncertainties are shown in Table 2. By considering the most probable value for the sample-to-sample uncertainty, as discussed above, the range of uncertainties for the weighted means at 95% confidence would reduce to 0.05–0.21 nm, exhibiting relative standard uncertainties ~1.4%. Some of the weighted means, given as the KCRVs in Table 2, change by 0.01 nm, whereas others remain unchanged.

From this work, it is now clear that XPS, on its own and if used carefully, has excellent precision and, for SiO<sub>2</sub> on Si, excellent linearity for thicknesses below 8 nm. However, XPS needs a calibration of the required attenuation length (a scaling parameter) *L*. This was carried out here in the pilot study P38 using a weighted average of the wavelength methods all directly traceable to the SI. In this way, the conventional XPS method has explicit traceability to the SI for SiO<sub>2</sub> on Si. The present data also confirm the pilot study P38 determination. For each new material system, a determination of the relevant attenuation length would be needed together with the extent of its constancy with thickness. With these numbers, all XPS instruments conforming to certain basic requirements and with valid software can then be used to analyse thicknesses in those material systems, traceably to the SI, using the reference procedures as established in the pilot study P38,<sup>[2]</sup> without further calibration. So this study provides an archetypal framework within which to model further ultra-thin film measurements. In their present state, the wavelength methods have excellent precision, linearity and accuracy, apart from their sensitivity to contamination that affects their offset values.

It is therefore clear that, for a wide range of materials in the sub-8-nm regime, the combination of XPS and one of the wavelength methods permits full and accurate measurements to be made of the amount of material, with a valid and accurate zero value. This does not necessarily require solution to the measurement of the offset and its uncertainty in the wavelength methods since one may simply determine the attenuation length, *L*, for XPS by using thickness differences. It should be repeated that the constancy of the attenuation length with thickness needs a careful evaluation for each material system. Alternatively, the wavelength method may be used if the contamination offset is determined by using the relationship to XPS. For the calibration by a wavelength method to be conducted reliably, the contamination on all samples needs to be as similar as possible. The present cleaning methods<sup>[2]</sup> do this adequately for relatively inert materials such as SiO<sub>2</sub>. With suitable experimental design, other thickness traceable methods, such as stylus methods<sup>[22]</sup>, transmission electron microscopy (TEM)<sup>[2,23]</sup> or XRF analysis,<sup>[24]</sup> not used in the present work, could also be added to the wavelength methods.

XPS as a conventional and popular method can be supported by primary (wavelength) methods by establishing a chain of traceability. After this calibration, because of the analytical capability and the lack of need to know and control the precise nature of the contamination, XPS will generally be the preferred method for analysis of ultra-thin films. In XPS, one only needs to transfer the attenuation length value for all XPS instruments, potentially, to have traceability. Wavelength methods may be supported by XPS in a way that their contamination offset can be corrected. After this correction, wavelength methods will be the preferred method for analysis of films >8 nm. There is an overlapping thickness range where both methods (after calibration/correction) may provide data for similar (high) quality. On the other hand, for films with quantities significantly lower than one monolayer, such as the contamination of Si wafers with metals, the length measure

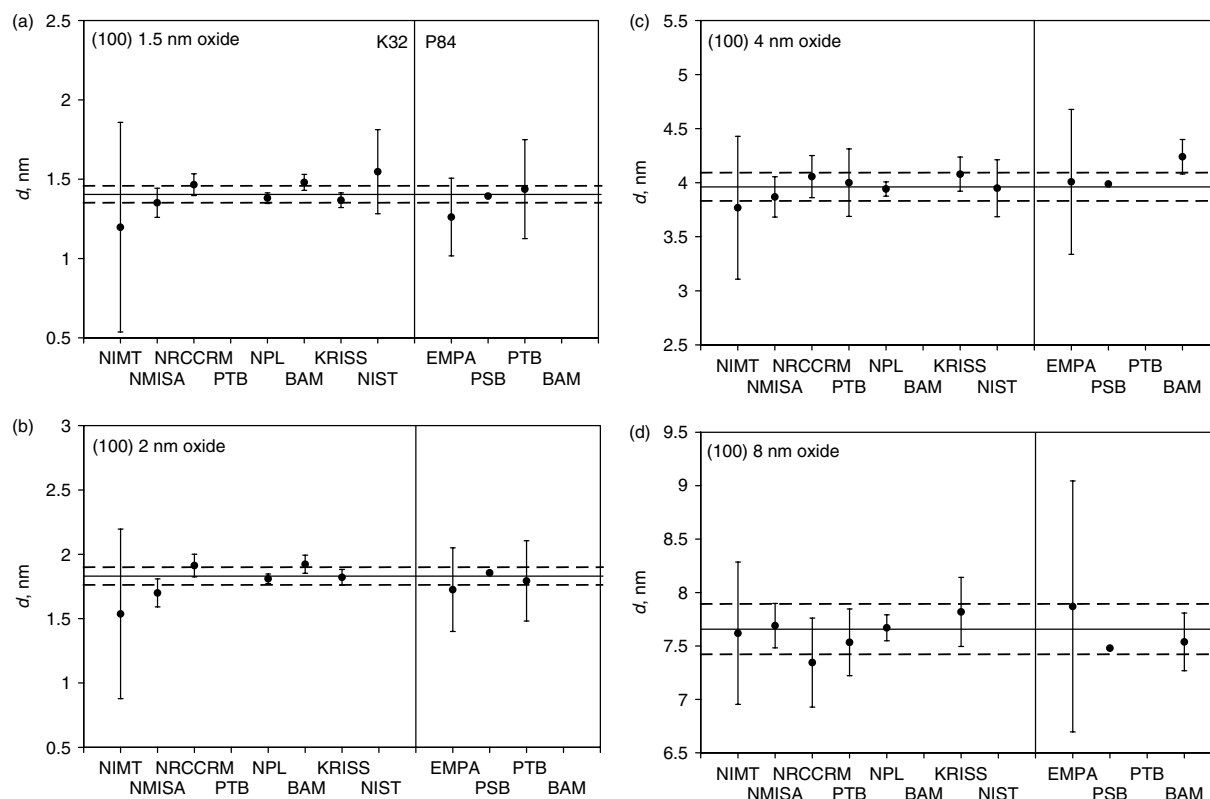


**Figure 4.** Measurements with their uncertainties as in Fig. 2, but using the reduced uncertainties discussed in the text, for the thicknesses of the (100) samples; (a) 1.5 nm, (b) 2 nm, (c) 4 nm and (d) 8 nm. The solid and dashed lines show the weighted average and the 95% confidence intervals, respectively.

becomes inappropriate and data are given in atoms/m<sup>2</sup>. For these, methods such as total reflection X-ray fluorescence (TXRF) or SIMS are used and calibration may be made by, for example, XRF or Rutherford backscattering spectrometry (RBS).

### Acknowledgements

The authors would like to thank M. G. Cox of NPL and S. J. Ellison of LGC for their helpful comments concerning the analysis of key comparisons, S. J. Spencer of NPL, M. Hoffmann of PTB, R. Leechaoen and A. Krajangmol of NIMT, T. Thongvijitmanee and S. Chareankij of the Thai Microelectronics Center, P. Chindaudom of the Thai National Electronics and Computer Technology Centre, P. A. Kienzie and C. J. Powell of NIST for their data and helpful discussions and D. Rosenthal of the Fritz Haber Institute (Max Planck Society) for discussions of dehydrogenation at SiO<sub>2</sub> surfaces. This work was supported under contract with the UK Department of Innovation, Universities and Skills within the National Measurement System Programme on Chemical and Biological Measurement. Certain commercial equipment, instruments or materials are identified in this paper to foster understanding. Such identification does not imply recommendation or endorsement by the authors or their Institutes, nor does it imply that the materials or equipments identified are necessarily the best available for the purpose.

### Appendix: Analysis of Uncertainties

In order to calculate the weighted average measured thickness for the KCRVs, it is important that the stated uncertainties include all

significant contributions with appropriate estimates. To analyse the uncertainties reported by each laboratory in detail, the measurement methods need a brief description. Below, we discuss the measurement uncertainty contributions in each method used in K32. The data for the associated P84 are included in the plots for information, but are not included in any of the calculations or discussions of the uncertainties.

#### X-ray photoelectron spectroscopy

The XPS method uses the intensities from the Si 2p peak for the SiO<sub>2</sub> and Si states,  $I_{\text{SiO}_2}$  and  $I_{\text{Si}}$ , respectively. If unmonochromated spectra are obtained, first the X-ray satellites are removed and then, in some cases to simplify the spectra, the spin-orbit splitting of 50% intensity at 0.60 eV higher binding energy can also be removed by deconvolution.<sup>[11]</sup> Where a monochromator is used, the satellite subtraction step is omitted. From these data, an equation often used to calculate the SiO<sub>2</sub> thickness,  $d$ , is

$$d = L \cos \theta \ln[1 + (I_{\text{SiO}_2}/R_0 I_{\text{Si}})] \quad (\text{A1})$$

where  $L$  is the attenuation length for the electrons measured in the SiO<sub>2</sub> overlayer, and  $R_0$  is the ratio of the intensities for bulk SiO<sub>2</sub> and bulk Si. This is known as the two-peak method. In the more commonly used and slightly more accurate formulation, the intensities of the interfacial oxides Si<sub>2</sub>O<sub>3</sub>, SiO and Si<sub>2</sub>O are also measured leading to a more complex set of equations given in Ref. [2].

These four thicknesses are then summed to give the effective SiO<sub>2</sub> thickness using the relation

$$d = d_{\text{SiO}_2} + 0.75 d_{\text{Si}_2\text{O}_3} + 0.5 d_{\text{SiO}} + 0.25 d_{\text{Si}_2\text{O}} \quad (\text{A2})$$

Equation (A2) apportions the thicknesses according to the oxygen content. The values of the  $L_{\text{Si}_2\text{O}_x}$  and  $R_{\text{Si}_2\text{O}_x}$  for  $x = 1$  to 3 are interpolated linearly between the values for SiO<sub>2</sub> and Si.<sup>[2,21]</sup> In the pilot study P38, it was noted that the three interfacial oxides contributed a thickness of  $0.128 \pm 0.008$  nm, close to the estimated 0.124 nm for an ideal interface.<sup>[2]</sup> The use of the simpler Eqn (A1) instead of Eqn (A2) does not lead to a difference as high as 0.128 nm since the fitting procedure with just two peaks leads to a slightly higher value of  $I_{\text{SiO}_2}$  than that obtained where five peaks are used.

In terms of the uncertainties for 95% confidence, the relevant relation is<sup>[25]</sup>

$$U^2 = U_E^2 + U_n^2 + U_\theta^2 + U_A^2 + U_P^2 + U_F^2 + U_L^2 \quad (\text{A3})$$

where  $U_n$ ,  $U_\theta$ , and  $U_A$  are terms for the laboratory's measurement statistics from the spectrometer signal, the angle setting and the analyser electron optics. The terms  $U_P$  and  $U_F$  are for the use of different numbers of peaks in the fitting of the data (as noted above) and the use of different peak shape algorithms.  $U_E$  is a term for the validity of the model and  $U_L$  is the uncertainty in the attenuation length. The value of  $U_n$  may depend on the individual analysis and  $U_\theta$  may be different for the (100) and (111) samples.  $U_n$  and  $U_\theta$  have random, type A, contributions whereas the other terms largely involve systematic type B contributions.

For the analysis conducted using the reference geometry established by NPL,<sup>[11]</sup>  $U_E$  is less than 0.025 nm,<sup>[22,26]</sup>  $U_A$  is negligible for an analyser cone entrance semi-angle  $< 6^\circ$ ,<sup>[27]</sup>  $U_P$  and  $U_F$  are negligible for fitting five peaks using valid software,<sup>[27]</sup> and, if  $R_o$  is taken as 0.9329, then  $U_L$ , determined in the pilot study P38,<sup>[21]</sup> is  $0.0107d$  at an expansion of  $k = 2$  for  $L$  taken as 2.996 or 3.485 nm for Mg or Al K $\alpha$  X-rays, respectively. The uncertainty in  $R_o$  is accommodated in this expression. The remaining terms depend on the statistical quality of the data recorded.

At NPL, the above procedure with five peaks, X-ray satellite and spin-orbit peak removal, was used for Mg K $\alpha$  X-rays with the magic angle geometry. In addition, repeated analyses of 22 different (100) and (111) samples showed that the random components of  $U_n$  and  $U_\theta$  gave contributions of  $0.00769d$  and  $0.00508d$  for (100) and (111) samples, respectively, with these values dominated by  $U_\theta$ . The difference for (100) and (111) surfaces is expected from the  $0.35^\circ$  estimated precision of setting the respective values of  $\theta$ . In addition to this is the accuracy of setting  $\theta$  and the standard uncertainty for this was shown earlier<sup>[13]</sup> to be significantly less than the value of  $0.35^\circ$  used for this comparison. This value was expanded to  $0.7^\circ$  at  $k = 2$  for 95% confidence. Use of these uncertainties leads directly to the values reported. An issue that also needs discussion is the zero origin of the relation for  $d$ . For clean Si,  $d$  should be zero but this will not be observed with zero uncertainty as a result of statistical noise in the background where the peak should be. That  $U_E$  is 0.025 nm is confirmed for  $d > 0.2$  nm in Refs [20,21] and for the range down to 0.022 nm in Ref. [26].

At NRCCRM, the same experimental and data reduction procedure, X-rays, reference geometry and value for  $R_o$  were used; however,  $L$  has been taken as  $2.964$  nm<sup>[2]</sup> instead of the later value of  $2.996$  nm<sup>[13]</sup> and the peak fitting was conducted

using six peaks without spin-orbit subtraction instead of five peaks after spin-orbit subtraction. The parameters  $U_F$ ,  $U_P$  and  $U_A$  were estimated to be in the range 0.2–1.3% for the nine samples. The random parts of  $U_n$  and  $U_\theta$  were estimated from six repeated measurements with the mean being reported. The samples were repositioned each time. The standard deviations of these six measurements, in the range 0.49–0.97%, were used for the unexpanded part of  $U_n$  and  $U_\theta$ . This is a valid expression for a typical measurement which is how some participants view a key comparison. Another valid approach is to use the standard deviation of the mean which would reduce this contribution by a factor of  $\sqrt{N}$ , where  $N = 6$ . This is valid for understanding the uncertainty of the final result. Dominating all these contributions is an estimated standard uncertainty of 2% for the absolute value of the emission angle  $\theta$ . The final standard uncertainties are all in the range 2.3–2.9%. These values are all expanded using  $k = 2$ . If the later value of  $L$  is used, the reported values would all scale up by a factor of 1.011 – a factor well within the stated uncertainties. In Fig. 3 and the revised data in Fig. 4, the  $L$  value has been taken as 2.996 to show, in a consistent way, what is attainable.

At NMISA, the same general procedure is applied except that now the Al K $\alpha$  X-rays are obtained from a monochromator so that the higher value of  $L_{\text{SiO}_2}$ , 3.485 nm, is used. The geometry is again the NPL reference geometry but this time the spin-orbit splitting is not subtracted but, instead, six peaks are fitted; two for the Si 2p elemental peak and one each for the remaining oxide states. Analysis shows that the likely error for this procedure is typically a standard uncertainty around 0.25%. Instead of using Eqn (A2), a simpler equation

$$d = L_{\text{SiO}_2} \cos \theta \times \ln \left[ 1 + \frac{I_{\text{SiO}_2} + 0.75 I_{\text{Si}_2\text{O}_3} + 0.5 I_{\text{SiO}} + 0.25 I_{\text{Si}_2\text{O}}}{R_o (I_{\text{Si}} + 0.75 I_{\text{Si}_2\text{O}} + 0.5 I_{\text{SiO}} + 0.25 I_{\text{Si}_2\text{O}_3})} \right] \quad (\text{A4})$$

is applied. This equation gives a result within a standard uncertainty of 0.6% of Eqn (A2).<sup>[25]</sup> The uncertainties are evaluated according to a version of Eqn (A3).  $U_E$  is taken as 0.025 nm, and the random parts of  $U_n$  and  $U_\theta$  are deduced from three measurements for each oxide thickness. Here, the uncertainty is taken as  $k$  times the standard deviation of the mean with  $k = 2$ . The type B part of  $U_\theta$  is estimated from a contribution of  $2^\circ$  with a rectangular distribution. Contributions of 5% have also been added for the statistical uncertainty of the low count levels of the main peaks  $I_{\text{SiO}_2}$  and  $I_{\text{Si}}$  in this monochromated instrument, 1% for the layer thickness homogeneity and 0.023 for the uncertainty in  $R_o$ , all from rectangular distributions. These give expanded values by first dividing by 1.73 (for the rectangular distribution) and then multiplying by 2. The added statistical uncertainty in the intensities is already reflected roughly in the standard deviation of the means of the three measurements. The layer thickness homogeneity is an uncertainty that is separately added, as already discussed, and the uncertainty in  $R_o$  is already subsumed into that for  $L$ . The final uncertainty estimates thus partially included some aspects twice and thus include a margin of safety. In Fig. 3 and the revised data in Fig. 4, these effects are removed to show, in a consistent way, what is attainable.

At BAM, the same experimental procedure, X-rays, reference geometry and values for  $L$  and  $R_o$  were used as in NPL. The input lens was stopped down to a semi-angle of  $6^\circ$  and seven measurements were made on each sample. The calculational procedure used Eqn (A2) but with six peaks after satellite subtraction, as at NMISA. The uncertainties from Eqn (A3) are taken with  $U_E$ ,  $U_A$ ,  $U_P$  and  $U_F$



as zero,  $U_L$  as 1.068%,  $U_n$  from the seven measurements with 1.0% contribution to the major two intensities and a total of  $2^\circ$  and 0.8% added linearly for the geometry and forward focussing in  $U_\theta$ , all at  $k = 2$ . This was all combined to give a total of 3.68% at  $k = 2$ , evaluated for the 1.5 nm (100) sample. This value was then applied to all samples. For the key comparison, this is valid since the three samples analysed were all of similar thicknesses.

At KRIS, the same experimental and data reduction procedure, X-rays, reference geometry and values for  $L$  and  $R_0$  were used as in NPL but only the (100) samples were analysed. Great care was taken to set the angles accurately with a laser system as described in Ref. [13]. Analyses were made with the five-peak procedure with spin-orbit splitting on all peaks. Three measurements were made on each sample with repositioning. The uncertainty estimate is made from Eqn (A3) with  $U_E$ ,  $U_A$ ,  $U_P$  and  $U_F$  as zero, and with  $U_L$  as 1.08%,  $U_n$ , from the standard deviation of the means for the three measurements, is typically 2%. The expanded uncertainty of  $2.4^\circ$  for the angle setting gives  $U_\theta = 2.84\%$ . These values are all at  $k = 2$  and give the total expanded Type B uncertainty of 3.04%, whereas the type A uncertainty ranges from 1.22 to 2.79%. These give the reported uncertainties.

### X-ray reflectometry

In XRR, the defining equation for the interference relation is given by

$$n\lambda = 2d \sin \theta \quad (\text{A5})$$

where  $\lambda$  is the X-ray wavelength,  $n$  the order of the interference and  $\theta$  the angle of incidence of the X-rays from the sample surface. In Eqn (A5), the terms are for parameters inside the layer. For parameters outside the layer, a small allowance for the refractive index of the layer is included. For a single film, as  $\theta$  is scanned, characteristic minima are observed with increasing order  $n$  with a separation defined by the above relation. For additional films, extra minima are superimposed at the relevant  $\theta$  values. In addition to the minima, the strength of the scattering, the reflectivity, is calculated from the atomic constituents and the density so that the whole of the intensity profile is calculated for a range of reflection angles. Although surface and interface roughness only affect the intensity, contamination layers may also affect the minima positions. These contributions may be included in the model. The model and reflectivity data are matched by a least squares analysis to deduce relevant parameters. Unlike XPS, XRR can measure thicknesses significantly greater than 8 nm, and, at these thicknesses, can make measurements on multi-layer samples. The precision of the method reduces as the films get thinner since there are fewer minima and, for the thinnest films used here, there is only one minimum in the range of data. For  $\text{SiO}_2$  on Si, using commercial XRR equipment,<sup>[28,29]</sup> the minima are not absolute minima in the reflectivity, but are relative minima when measured against the general trend of data. XRR does not provide a direct chemical analysis and fitting of the reflectance data is conducted for trial models. Exactly what is fitted depends on the available software.

For XRR, PTB used the BESSY II electron storage ring, as this enables the selection of the X-ray energy at 1841 eV to optimise contrast between the optical constants of  $\text{SiO}_2$  and Si. This analysis is conducted in vacuum. At this energy, the minima are deep and sharp<sup>[2]</sup> and the use of vacuum reduces the contamination. Here, the total uncertainty at 95% confidence, with  $k = 2$ , is 0.10 nm for all samples. In addition, the observation of the offset of 0.49 nm, observed earlier,<sup>[2]</sup> was considered, and XRF measurements at

480 eV showed that a layer of carbon,  $0.21 \pm 0.02$  nm in thickness, was on the surface. The expanded uncertainty for the carbon, 0.02 nm, was linearly added to the 0.10 nm for the measurement accuracy. However, in subtracting the total contamination offset of 0.49 nm, given in Table 1, derived from the pilot study P38, this separate contribution ( $0.21 \pm 0.03$  nm) is ignored in determining the KCRV shown in Table 2. The uncertainties are added in quadrature. Studies are being performed to distinguish between contamination layers and the oxide layer by XRR measurements at several photon energies around the K absorption edges for silicon and oxygen. These results will be presented elsewhere.

### Neutron reflectometry

The basic principle of NR is very similar to XRR, but the use of neutrons gives a scattering related to the scattering cross section of the atomic nucleus rather than the effective  $Z$  of the electron cloud. This method, as above, is conducted in vacuum. Thus, Eqn (A5) is valid and, again, the whole of the reflectivity curve is modelled for a depth profile of the SLD, including the surface and interface roughness. The model and data are matched by a least squares analysis to deduce relevant parameters. The uncertainties are deduced from the range of the values of the given parameter from all valid models returned by least squares refinement and are given at a level of 95% confidence. The reported values include an expanded uncertainty contribution of 0.21%, at a confidence level of 95%, in the neutron wavelength. The uncertainty for the angle of incidence is negligible. In the pilot study P38<sup>[2,19]</sup> the data were shown to exhibit an offset of 0.22 nm with respect to the XPS data, and a similar offset also appears here. In general, distinct contamination layers would show up in the SLD profiles determined by NR. However, simulations of NR reflectivities demonstrate that, if the SLD values for proposed contamination layers are within  $\pm 15\%$  of the  $\text{SiO}_2$  SLD, the contamination is indistinguishable from  $\text{SiO}_2$ . Thus if the composition and density of the contamination were to result in an SLD within this range, the measured thickness of  $\text{SiO}_2$  would include such a contamination layer. In order to match the SLD of  $\text{SiO}_2$  with carbon containing contamination, the density and composition would have to be relatively large. One candidate that would satisfy these conditions due to its high atomic density and lack of hydrogen (which has a negative scattering length) is a carbon layer as proposed earlier with a density that is similar to that of graphite, at a roughly half a monolayer coverage. The offset given in Table 1, determined from the pilot study P38, is thus subtracted from the original data to give the value used in the KCRV and shown in Table 2. The uncertainties are added in quadrature.

### Ellipsometry

The principle of ellipsometry is similar to that of XRR in that the light reflectance intensities are measured, but here the similarities end. The method is conducted in air and that has advantages of speed and, for delicate samples, sample integrity. In its most basic terms an ellipsometer measures, under specular reflection conditions, the change in the phase difference between the parallel and perpendicular components of the light beam upon reflection,  $\Delta$ , and the ratios of the outgoing wave amplitudes to the incoming wave amplitudes for these components, respectively. The ratio of the latter gives  $\tan \Psi$  and it is  $\Delta$  and  $\Psi$  that are generally measured. For  $\text{SiO}_2$  films, in  $\Delta$ ,  $\Psi$  space has been reported<sup>[30]</sup> that at one wavelength, the co-ordinates form a trajectory starting from

$\Delta \approx 178.5^\circ$ ,  $\Psi = 10.5^\circ$ , moving, approximately, in an elliptical manner anti-clockwise. For films up to 10-nm in thickness, the trajectory is towards  $\Delta = 150^\circ$  with less than a degree change in  $\Psi$ . The precise trajectory in  $\Delta$ ,  $\Psi$  space may be calculated using the known optical constants for the SiO<sub>2</sub> overlayer and the Si substrate. Thus, for a perfect layer of SiO<sub>2</sub> on Si, all of the optical parameters are known and the thickness may be determined. Issues that are not easy to address are the effects of the interface oxides that may be small, and of the contamination overlayers, which are generally unquantified.

At NIMT, a simple three-layer model was used for air, SiO<sub>2</sub> and Si with optical properties taken from the database supplied by the instrument manufacturer. A number of test measurements were made leaving the samples contaminated with hydrocarbons. The amount of these contaminants was reduced with IPA, as suggested in the key comparison protocol. To remove contaminants further, the heating method of NIST was used. The samples were heated to 350 °C for 10–15 min and then allowed to cool for 10–15 min prior to measurement. On each sample, five locations were measured with three repetitions at each location. This whole set of data was repeated twice more on different days, leading to a total of 45 measurements for each sample. Measurements just before and just after the heating showed a thickness reduction of 0.33 nm. Measurements comparing the first data recorded and that after cleaning showed a reduction of 0.26 nm. The materials just prior to heating were significantly more contaminated than those in the original measurements and required cleaning with IPA as noted above. These thickness reductions are consistent with those seen for this heating in the pilot study P38.<sup>[2]</sup>

The ellipsometry data give plots of  $\Delta$  and  $\Psi$  for the two wavelengths as a function of the angle of incidence and these curves are matched to model curves with the thickness as a variable. Experimentally, it is found, as expected, that  $\Psi$  changes little for  $d < 10$  nm so that the fitting is mainly for  $\Delta$ . Data for the fitting in all samples show a standard uncertainty of 0.263 nm in each fit to the model in each measurement. This is deduced from the change in  $d$  required to increase the reduced  $\chi^2$  by unity where the reduced  $\chi^2$  is determined from the difference between the data and the fitted model. Analyses of all the data lead to further standard uncertainties of 0.004 nm for the measurement repeatability, 0.012 nm for the sample uniformity and 0.028 nm for the day-to-day repeatability. The uncertainty of the optical wavelengths has an insignificant effect. The uncertainty in the optical constants for the oxide is important for  $n_{\text{opt}}$  but not for  $k_{\text{opt}}$ , as it is zero. Extremities for  $n_{\text{opt}}$  for SiO<sub>2</sub> are 1.45 and 1.47. There are similar extremes for Si for both  $n_{\text{opt}}$  and  $k_{\text{opt}}$ . When all these terms are appropriately added in quadrature, the final uncertainties are similar to the uncertainty for the fit and, when expanded, the average is 0.533 nm. The fit uncertainty is thus important. It is a type B uncertainty and one that does not reduce with an increase in the number of measurements. This uncertainty estimate will mainly include contributions from the inadequacy of the model. In the pilot study P38,<sup>[2]</sup> it was interpreted that the adventitious carbonaceous contamination, adsorbed water, etc., led to offsets in the range 0.45–1.24 nm with an average difference for measurements of packaged samples of 1.01 nm with a standard uncertainty of 0.04 nm. It was also shown that the heating used in one case led to a reduction of only 0.23 nm, with a standard deviation of the mean of 0.03 nm, from 1.22 nm. In a heating study at NPL,<sup>[2]</sup> XPS measurements showed the carbon thickness reduced from 0.2 to 0.1 nm, but in no cases have the contaminations been completely removed. No XPS data are

available for the water contamination levels. The contamination offset evaluated in this way, from the pilot study P38 data, is shown in Table 1. This is subtracted to give the data used in calculating that shown in Table 2. The uncertainties are added in quadrature.

## References

- [1] *International Technology Roadmap for Semiconductors*, (2001 and 2002 editions), <http://public.itrs.net/>.
- [2] M. P. Seah, S. J. Spencer, F. Bensebaa, I. Vickridge, H. Danzebrink, M. Krumrey, T. Gross, W. Oesterle, E. Wendler, B. Rheinländer, Y. Azuma, I. Kojima, N. Suzuki, M. Suzuki, S. Tanuma, D. W. Moon, H. J. Lee, H. M. Cho, H. Y. Chen, A. T. S. Wee, T. Osipowicz, J. S. Pan, W. A. Jordaan, R. Hauert, U. Klotz, C. Marel, M. Verheijen, Y. Tamminga, C. Jeynes, P. Bailey, S. Biswas, U. Falke, N. V. Nguyen, D. Chandler-Horowitz, J. R. Ehrstein, D. Muller, J. A. Dura, *Surf. Interface Anal.* **2004**, 36, 1269.
- [3] A. Picard, *Metrologia* **2006**, 43, 46.
- [4] P. Becker, H. Bettin, H.-U. Danzebrink, M. Gläser, U. Kuetgens, A. Nicolaus, D. Schiel, P. De Bièvre, S. Valkiers, P. Taylor, *Metrologia* **2003**, 40, 271.
- [5] R. W. Roberts, T. A. Vanderslice, *Ultrahigh Vacuum and its Applications*, Prentice Hall: USA, **1963**.
- [6] D. A. Cole, J. R. Shallenberger, S. W. Novak, R. L. Moore, M. J. Edgell, S. P. Smith, C. J. Hitzman, J. F. Kirchhoff, E. Principe, W. Neiveen, F. K. Huang, S. Biswas, R. J. Bleiler, K. Jones, *J. Vac. Sci. Technol., B* **2000**, 18, 440.
- [7] M. P. Seah, *Metrologia Tech. Suppl.* **2008**, 45, 08013, DOI: 10.1088/0026-1394/45/1A/08013, linking to BIPM website for NPL Report AS 27 also directly at: [http://www.bipm.org/utis/common/pdf/final\\_reports/QM/K32/CCQM-K32.pdf](http://www.bipm.org/utis/common/pdf/final_reports/QM/K32/CCQM-K32.pdf) or from NPL at <http://publications.npl.co.uk/npl-web/pdf/as27.pdf>.
- [8] *International Vocabulary of Basic and General Terms in Metrology* (2nd edn), ISO: Geneva, **1993**.
- [9] ISO 17025, *General Requirements for the Competence of Testing and Calibration Laboratories*, ISO: Geneva, **2005**.
- [10] M. P. Seah, R. White, *Surf. Interface Anal.* **2002**, 33, 960.
- [11] M. P. Seah, S. J. Spencer, *Surf. Interface Anal.* **2002**, 33, 640.
- [12] M. P. Seah, S. J. Spencer, *J. Vac. Sci. Technol., A* **2003**, 21, 345.
- [13] M. P. Seah, S. J. Spencer, *Surf. Interface Anal.* **2005**, 37, 731.
- [14] J. A. Dura, D. J. Pierce, C. F. Majkrzak, N. C. Maliszewskyj, D. J. McGillavray, M. Lösche, K. V. O'Donovan, M. Mihailescu, U. Perez-Salas, D. L. Worcester, S. H. White, *Rev. Sci. Instrum.* **2006**, 77, 074301.
- [15] J. A. Dura, C. A. Richter, C. F. Majkrzak, N. V. Nguyen, *Appl. Phys. Lett.* **1998**, 73, 2131.
- [16] V. M. Guńko, R. Leboda, Carbon-silica adsorbents, in *Encyclopedia of Surface and Colloid Science* (2nd edn) (Eds: P. Somasundaran, A. Hubbard), Taylor & Francis: London, New York, **2006**, p 1120.
- [17] S. Mizushima, *Metrologia* **2004**, 41, 137.
- [18] A. Picard, H. Fang, *Metrologia* **2004**, 41, 333.
- [19] S. Mizushima, *Metrologia* **2005**, 42, 208.
- [20] Y. Azuma, J. Fan, I. Kojima, S. Wei, *J. Appl. Phys.* **2005**, 97, 123522.
- [21] M. P. Seah, Supplementary data on uncertainties in XPS and updated tables for the CCQM pilot study, P38, of thickness measurements for ultra-thin SiO<sub>2</sub> on Si, *NPL Report DQL-AS(RES) 010*, March **2005**.
- [22] P. Thomsen-Schmidt, K. Hasche, G. Ulm, K. Herrmann, M. Krumrey, G. Ade, J. Stümpel, I. Busch, S. Schädlich, A. Schindler, W. Frank, D. Hirsch, M. Procop, U. Beck, *Appl. Phys., A* **2004**, 78, 645.
- [23] K. J. Kim, Y.-S. Kim, J. S. Jang, J. W. Kim, K. W. Kim, *Metrologia* **2008**, 45, 507.
- [24] M. Kolbe, B. Beckhoff, M. Krumrey, G. Ulm, *Spectrochim Acta* **2005**, 60, 505.
- [25] M. P. Seah, S. J. Spencer, *Surf. Interface Anal.* **2003**, 35, 515.
- [26] K. J. Kim, M. P. Seah, *Surf. Interface Anal.* **2007**, 39, 512.
- [27] M. P. Seah, *Surf. Interface Anal.* **2005**, 37, 300.
- [28] I. Kojima, L. Boquan, *The Rigaku Journal* **1999**, 16, 31.
- [29] I. Kojima, B. Li, T. Fujimoto, *Surf. Interface Anal.* **1999**, 28, 267.
- [30] H. G. Tomkins, E. A. Irene, *Handbook of Ellipsometry*, Springer: Berlin, **2004**.